Azerbaijan University of Architecture and Construction
ISSN 2706-7726
Engineering Mechanics
Scientific and Technical Journal
E-mail: engineeringmechanics@azmiu.edu.az

December 2025	Issue 22	Volume 14	Number 4	Pages 33-39

NUMERICAL MODELLING OF NONLINEAR WAVES IN FLUID-SATURATED POROUS MEDIA

Musraddin TAGHIYEV, Ayla ALIYEVA
Baku State University, Faculty of Mechanics and Mathematics
tagiyev.misir@gmail.com, ayla20020609@gmail.com

Abstract: *The model proposed in this study describes the propagation of nonlinear waves in two-phase media while accounting for thermodynamic forces. The formulated mathematical problem was complemented by equations expressing the conservation of mass and momentum for each phase, the rheological equation of the solid phase, and thermodynamic relations. A one-dimensional problem was considered and was solved using the method of small parameters. As a result, a dispersion relation and an evolution equation with Korteweg–de Vries–type nonlinearity were obtained. The resulting equation was solved numerically, and the results were analyzed.*

Keywords: *fluid, wave, phase, porosity, medium, velocity.*

Mathematical modelling plays a significant role in the study of nonlinear wave theory. It enables the prediction and optimization of technological effects, as well as the interpretation and processing of experimental data [4]. In this regard, the present work investigates the propagation velocities of longitudinal waves and changes in the profiles of nonlinear waves in fluid-saturated porous media under impulsive loading.

It is shown that the generated disturbance is transported by two distinct waves propagating at different velocities. It should be noted that the dependence of the deformation of each wave on the parameters of the problem has been investigated. The proposed models describe the processes of nonlinear wave propagation in fluid-saturated porous media (here one phase is solid and the other is fluid) [1–2].

Initially, each equation of the system describing the considered process is rewritten in terms of new variables. The resulting system of equations was solved jointly. The sought functions were represented in series form. Solving the formulated problem using the method of small parameters, a dispersion relation

expressed by a biquadratic equation were obtained in the first approximation [2]:

$$\alpha_1^{(0)}\rho_1^{(0)}b_0\left[\alpha_1^{(0)}\rho_2^{(0)}(L_1 - D_1\gamma) + \rho_1^{(0)}\alpha_2^{(0)}B_1\right]c^4 + \left[\alpha_1^{(0)}\rho_2^{(0)}\left(\alpha_1^{(0)}a_0D_1 - \right.\right.$$
$$\left.\left. - a_0L_1 + \alpha_1^{(0)}\rho_1^{(0)}b_0 - \gamma\rho_1^{(0)}b_0\right) + \rho_1^{(0)}\alpha_2^{(0)}\left(\alpha_1^{(0)}\rho_1^{(0)}b_0 - a_0B_1\right)\right]c^2 -$$
$$- \rho_1^{(0)}\alpha_2^{(0)}a_0 = 0. \qquad (1)$$

Here , $B_1 = \rho_2^{(0)}\beta_2$, $L_1 = \frac{\rho_1^{(0)}}{3}\beta_1$, $D_1 = \frac{\rho_1^{(0)}}{3\alpha_1^{(0)}}\beta_1$, $L_2 = D_2 = 0$, $\alpha_1^{(0)}$, $\alpha_2^{(0)}$ – denote the initial concentrations of the solid and fluid phases, $\rho_1^{(0)}$, $\rho_2^{(0)}$ - the initial densities of the solid and fluid phases, a_0 , b_0 – constant determined on the basis of specific viscoelastic models [3]. β_1 represents the isothermal compressibility coefficient of the solid.

The dispersion equation (1) has two real roots. The first root corresponds to the wave velocity in the fluid phase, while the second root represents the wave velocity in the solid phase. The wave velocities were calculated for various parameter values, and the results are presented in tables. The following data were used in the calculations:

$\rho_2^{(0)} = 10^{-6}\frac{kg\cdot s^2}{sm^4}$, $\beta_2 = 4\cdot 10^{-5}\frac{sm^2}{kg}$, in the solid skeleton

$\rho_1^{(0)} = 2{,}5\cdot 10^{-6}\frac{kg\cdot s^2}{sm^4}$, $\beta_1 = 2\cdot 10^{-5}\frac{sm^2}{kg}$, $E_1 = 10^5\frac{kg}{sm^2}$, $\nu = 0{,}3$

Additionally, in Table 2, the following data were also used:

$$\alpha_2^{(0)} = 0{,}1\ , E_1 = 10^4\frac{kg}{sm^2}\ , \nu = 0{,}2\frac{sm^2}{s}$$

From Table 1 and 2 it is evident that, for fixed values of other parameters, an increase in porosity $\alpha_2^{(0)}$ as well as an increase in the compressibility coefficient of the solid phase β_1 leads to a monotonic increase in the wave velocity in the fluid phase, whereas the wave velocity in the solid phase decreases. The calculations also show that a simultaneous increase in Poisson's ratio and the density of the solid phase results in a decrease in the wave velocity in the skeleton. In this case, the change in the wave velocity in the fluid phase is negligible. The propagation velocities of waves in both phases have also been studied for various values of other parameters.

Table 1

$\alpha_2^{(0)}$	0,05	0,1	0,2
$c_1\left(\frac{m}{s}\right)$	693	908	1151
$c_2\left(\frac{m}{s}\right)$	4167	3426	2999

Table 2

$\beta_1\left(\frac{sm^2}{kg}\right)$	10^{-6}	$2 \cdot 10^{-6}$	10^{-5}	$5 \cdot 10^{-5}$
$c_1\left(\frac{m}{s}\right)$	858	861	888	1129
$c_2\left(\frac{m}{s}\right)$	3749	3613	2873	1533

Table 3

$\rho_1^{(0)}\left(\frac{kg \cdot s^2}{sm^4}\right)$	$1{,}5 \cdot 10^{-6}$	$2{,}5 \cdot 10^{-6}$	$2{,}5 \cdot 10^{-6}$	$3{,}5 \cdot 10^{-6}$
$\beta_1\left(\frac{sm^2}{kg}\right)$	$5 \cdot 10^{-6}$	$2 \cdot 10^{-6}$	$2 \cdot 10^{-6}$	10^{-6}
$E_1\left(\frac{kg}{sm^2}\right)$	10^4	10^5	10^5	$2{,}5 \cdot 10^5$
$\nu\left(\frac{sm^2}{s}\right)$	0,2	0,25	0,3	0,3
$c_1\left(\frac{m}{s}\right)$	890	876	907	895
$c_2\left(\frac{m}{s}\right)$	4142	3563	3415	3060

Table 4

$\rho_2^{(0)}\left(\frac{kg \cdot s^2}{sm^4}\right)$	$2 \cdot 10^{-6}$	10^{-6}	$3 \cdot 10^{-9}$	10^{-9}

$\beta_2\left(\frac{sm^2}{kg}\right)$	$4\cdot10^{-6}$	$4\cdot10^{-5}$	10^{-1}	0,8
$c_1\left(\frac{m}{s}\right)$	729	861	577	353
$c_2\left(\frac{m}{s}\right)$	6491	3613	2109	2108

Table 4 presents the regularities governing the dependence of acoustic wave propagation velocities c_1 and c_2 on the physical and mechanical properties of the fluid ($E_1 = 10^4\ kg/m^2,\ \nu = 0{,}2$).

The analysis shows that the velocity of c_2 type acoustic waves propagating in the skeleton of a porous medium directly depends on the parameters of the fluid saturating the solid phase. This effect is more pronounced for fluids than for gases (Table 5). When the formation is saturated with gas, the influence of the solid phase (skeleton) on the propagation velocity of c_1 type acoustic waves becomes almost negligible. This result was obtained for the following parameter values:

$$\rho_2^{(0)} = 10^{-9}\ kg\cdot s^2/sm^4,\ \alpha_2^{(0)} = 0{,}2,\ \beta_1 = 2\cdot10^{-6}\ sm^2/kg$$

.

Table 5

$\rho_1^{(0)}\left(\frac{kg\cdot s^2}{sm^4}\right)$	$1{,}5\cdot10^{-6}$	$2{,}5\cdot10^{-6}$	$3{,}5\cdot10^{-6}$
$\beta_1\left(\frac{sm^2}{k}\right)$	$5\cdot10^{-6}$	$2\cdot10^{-6}$	10^{-6}
$E_1\left(\frac{k}{sm^2}\right)$	10^4	$5\cdot10^4$	10^5
$\nu\left(\frac{sm^2}{s}\right)$	0,2	0,25	0,3
$c_1\left(\frac{m}{s}\right)$	353	353	353
$c_2\left(\frac{m}{s}\right)$	2722	2108	1782

From Table 4 it follows that the wave velocity in the skeleton depends on ($E_1 = 10^4\ kg/m^2,\ \nu = 0{,}2$) the properties of the fluid saturating the solid phase, which determine the distribution patterns of acoustic wave c_1 and c_2 velocities.

In this work, wave velocities in sandstones, limestones, and quartz sands saturated with formation water were also determined, and the results were

presented in the following table:

Table 6

	$Sandstones$	$Limestones$	$Quartz\ sands$
$\rho_2^{(0)}\left(\frac{kg\cdot s^2}{sm^4}\right)$	10^{-6}	10^{-6}	10^{-6}
$\beta_2\left(\frac{sm^2}{kg}\right)$	$4{,}4\cdot 10^{-5}$	$4{,}4\cdot 10^{-5}$	$4{,}4\cdot 10^{-5}$
$c_1\left(\frac{m}{s}\right)$	1053	827	1238
$c_2\left(\frac{m}{s}\right)$	2913	3511	2862

In the second approximation, an evolution equation with Korteweg–de Vries– type nonlinearity was obtained:

$$\frac{\partial\vartheta}{\partial x}+\vartheta\frac{\partial\vartheta}{\partial T}-R_2\vartheta\left(1+\frac{r}{|R_1|}\left|1-\frac{\alpha_1^{(0)}\rho_1^{(0)}-a_0(b_0c^2)}{\rho_1^{(0)}\left(\alpha_1^{(0)}-\gamma\right)}\right||\vec{\vartheta}|\right)+R_3\sum_{l=1}^{n}(-1)^{l+1}A_{l+1}\frac{\partial^{l+1}\vartheta}{\partial T^{l+1}}=0 \qquad (2)$$

where

$$A_{l+1}=\left(\Gamma_{m-l}\frac{a_0b_l}{b_0}-\Gamma_{n-l}a_l\right),T=c^{-1}x-t.$$

It should be noted that when , $m=3$ and $n=5$, a solution of the equation (2) satisfying the conditions

$$\vartheta(0,t)=-R_1e^{-2t^2},\vartheta(-\infty,x)=\vartheta(\infty,x)=0,$$

$$\frac{\partial^{j-2}\vartheta}{\partial T^{j-2}}\Big|_{T=-\infty}=\frac{\partial^{j-2}\vartheta}{\partial T^{j-2}}\Big|_{\infty}=0\,;\ \frac{\partial^{n-1}\vartheta}{\partial T^{n-1}}\Big|_{T=-\infty}=0\,,j=3,4,5,$$

is obtained [1-2]. Numerical calculations were carried out for fluid-saturated sandstones and limestones, corresponding graphs were constructed, and the results were compared.

Here ,

$$R_1 = \frac{\alpha_2^{(0)}(1+c^2B_1)}{c\rho_2^{(0)}\left(\alpha_1^{(0)}-\gamma\right)^2}\left(\alpha_1^{(0)}\rho_1^{(0)}-\frac{a_0}{b_0c^2}\right)^2\left[\left(\alpha_1^{(0)}\rho_1^{(0)}-\frac{a_0}{b_0c^2}\right)\cdot\right.$$
$$\cdot\left(c^{-2}\rho_1^{(0)}-2\rho_2^{(0)}L_1+2\rho_1^{(0)}B_1\right)+\alpha_1^{(0)}\rho_2^{(0)}\left(2\rho_1^{(0)}\gamma-\frac{3a_0}{b_0c^2}\right)D_1$$
$$\left.-c^{-2}\alpha_1^{(0)}\rho_1^{(0)}\rho_2^{(0)}\right]+\frac{a_0\alpha_1^{(0)}\rho_1^{(0)}\rho_2^{(0)}}{b_0c^3}\left(\alpha_1^{(0)}D_1+c^{-2}\right)$$
$$+2c^{-3}\alpha_1^{(0)}\rho_1^{(0)}\rho_2^{(0)}\cdot\left(\alpha_1^{(0)}\rho_1^{(0)}-\frac{a_0}{b_0c^2}\right)$$
$$+2c^{-3}\frac{\alpha_2^{(0)}\rho_1^{(0)}}{\rho_2^{(0)}\left(\alpha_1^{(0)}-\gamma\right)^2}\left(\alpha_1^{(0)}\rho_1^{(0)}-\frac{a_0}{b_0c^2}\right)^3+\frac{2c\alpha_1^{(0)}\rho_2^{(0)}}{\left(\alpha_1^{(0)}-\gamma\right)^2}\cdot$$

$$\cdot\left(\alpha_1^{(0)}\rho_1^{(0)}-\frac{a_0}{b_0c^2}\right)\left[\alpha_1^{(0)}\alpha_1^{(0)}\left(\rho_1^{(0)}\gamma-\frac{a_0}{b_0c^2}\right)^2D_2-\alpha_1^{(0)}\left(\rho_1^{(0)}\gamma-\frac{a_0}{b_0c^2}\right)\cdot\right.$$
$$\cdot\left(\alpha_1^{(0)}\rho_1^{(0)}-\frac{a_0}{b_0c^2}\right)D_L+\left(\alpha_1^{(0)}\rho_1^{(0)}-\frac{a_0}{b_0c^2}\right)^2L_2$$
$$\left.+\frac{\alpha_2^{(0)}\rho_1^{(0)}}{\alpha_1^{(0)}\rho_2^{(0)}}\left(\alpha_1^{(0)}\rho_1^{(0)}-\frac{a_0}{b_0c^2}\right)^2B_2\right]/\Delta$$

$$R_2 = K_\nu\rho_2^{(0)}\left[\frac{a_0}{b_0^2c}\left(\alpha_1^{(0)}D_1+c^{-2}\rho_1^{(0)}/\rho_2^{(0)}\right)+c^{-2}\alpha_1^{(0)}\rho_1^{(0)}\left(1-\rho_1^{(0)}/\rho_2^{(0)}\right)\right]\cdot$$
$$\cdot\left(1-\frac{\alpha_1^{(0)}\rho_1^{(0)}-a_0/(b_0c^2)}{\rho_1^{(0)}\left(\alpha_1^{(0)}-\gamma\right)}\right)/\Delta$$

$$R_3 = \frac{\alpha_1^{(0)}\rho_1^{(0)}\rho_2^{(0)}}{b_0c^2}\left(\alpha_1^{(0)}D_1+c^{-2}\right)/\Delta$$

$$\Delta = 2c\alpha_1^{(0)}\rho_1^{(0)}\rho_2^{(0)}\left[\alpha_1^{(0)}\left(\frac{a_0}{b_0c^2}D_1+c^{-2}\rho_1^{(0)}\right)+\frac{c^{-2}\alpha_2^{(0)}}{\alpha_1^{(0)}\rho_2^{(0)}\left(\alpha_1^{(0)}-\gamma\right)}\cdot\left(\alpha_1^{(0)}\rho_1^{(0)}-\frac{a_0}{b_0c^2}\right)^2\right]$$

For the case $\Gamma_{n-l}=1$, $n\geq l$, $\Gamma_{n-l}=0$, $n<1$,

$$A_2 = -E_1\theta - E_*\theta_* ;$$
$$A_3 = -(E_1+E_*)\theta\theta_* - M_2 ;$$
$$A_4 = \frac{E_2}{E_1}M_1\theta-(M_1+M_2)\theta-\left(M_1+M_2\frac{E_2+E_*}{E_1}\right)\theta_* ;$$

$$A_5 = -M_1\left(\theta\theta_* + \frac{M_2}{E_1}\right);$$

$$A_6 = -\frac{M_1 M_2}{E_1}\theta_*;$$

Numerical calculations were performed for porous media such as fluid-saturated sandstones and limestones, using the additional data specified below:

$E_k = 10^3\,\frac{kg}{sm^2}$, $\theta = 10^{-1}s^{-1}$, $\theta_* = 10^{-2}s^{-1}$, $M_1 = 3\cdot 10^3\,\frac{kg\cdot s^2}{sm^2}$, $M_2 = 10^2\,\frac{kg\cdot s^2}{sm^2}$.

Figures 1–4 show that the input impulse is transported by two waves in a porous medium: one propagating in the fluid and the other in the skeleton.

In the considered case, Figure 1 shows that the propagation distance of the impulse in limestone $\left(k_\nu = 0{,}5\,\frac{kg\cdot s}{sm^3}\right)$ is greater than in sandstone $\left(k_\nu = 0{,}5\,\frac{kg\cdot s}{sm^3}\right)$ (Figure 3).

However, in sandstone the tensile impulse intensifies with increasing distance, the wave becomes compressed and attenuates rapidly. In the fluid phases of both limestone and sandstone, tensile impulses, without changing sign, shortens their propagation distance compared to the solid phase (Figures 2 and 4 versus Figures 1 and 3).

In equation (2), accounting for inertia forces characterized by the particle mass leads to wave attenuation during propagation. An increase in the interphase resistance coefficient is also always accompanied by wave attenuation in the medium. However, if the medium is gas-saturated, waves can propagate over long distances without changing their profile.

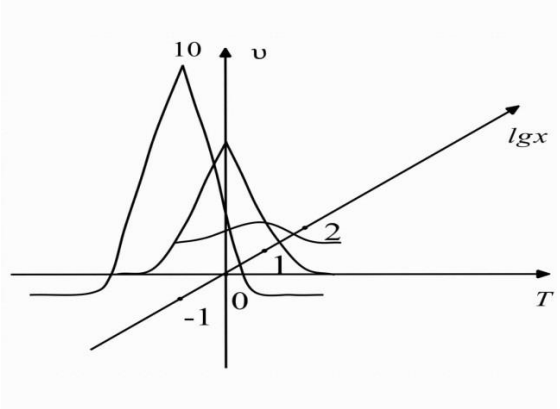

Figure 1

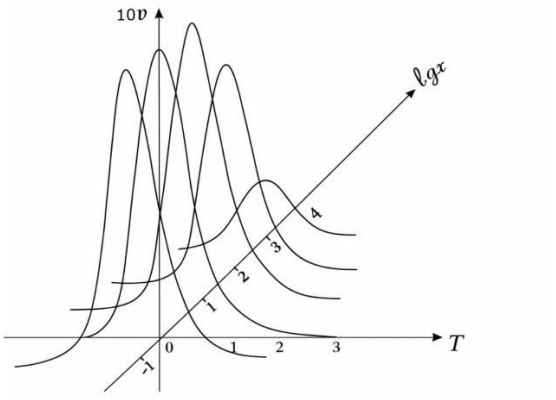

Figure 2

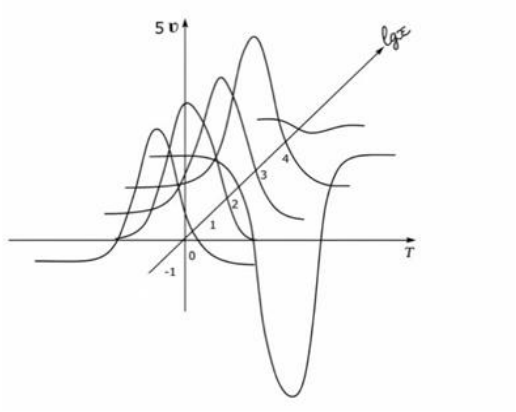

Figure 3

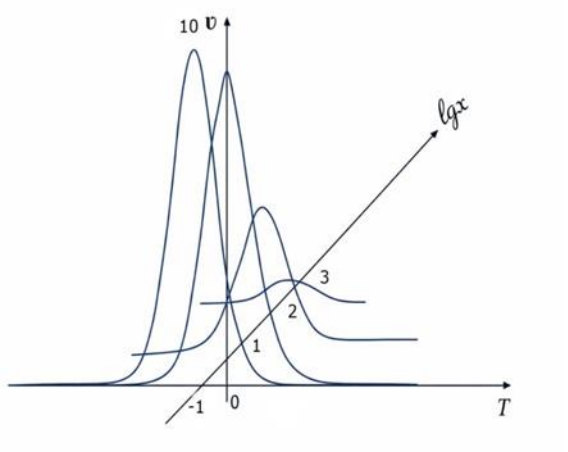

Figure 4

Ədəbiyyat

1. Ramazanov, T. K., & Kurbanov, A. I. (1995). The numerical modeling of nonlinear wave processes in two-phase systems. In Proc. Of the 26th Annual Iranian Mathematics Conference Kerman (pp. 341-346).
2. Рамазанов Т. К. , Курбанов А. И. , Тагиев М. М. Нелинейные волновые процессы в двух взаимопроникающих сжимающих средах. Сборник трудов I респиб. конфер. По механике и математике, Часть I, Механика, Баку, 1995, стр. 148-152.
3. Рамазанов, Т. К. (1995). Нелинейные волны в двухфазных системах. International Applied Mechanics, Киев, 31(8), 38-45.
4. Николаевский, В. Н. (1988). Нелинейные волны в грунтах и трещиноватых горных породах. Физ. тех. проб. разработки полозных ископаемых, (6-С), 31-38.